

THE CIRCUMGALACTIC ENVIRONMENT OF BRIGHT *IRAS* GALAXIES

Y. KRONGOLD AND D. DULTZIN-HACYAN

Instituto de Astronomía, Apartamentado Postal 70-264, Universidad Nacional Autónoma de México, 04510 Mexico DF, Mexico;
yair@astrocu.unam.mx, deborah@astrocu.unam.mx

AND

P. MARZIANI

Osservatorio Astronomico, INAF, Vicolo dell' Osservatorio 5, I-35122 Padua, Italy; marziani@pd.astro.it

Received 2001 October 18; accepted 2002 February 14

ABSTRACT

This paper systematically studies, for the first time, the circumgalactic environment of bright *IRAS* galaxies as defined in 1989 by Soifer and coworkers. While the role of gravitational interaction for luminous and ultraluminous *IRAS* galaxies has been well established by various studies, the situation is by far more obscure in the IR luminosity range of the bright *IRAS* sample, $10^{10} L_{\odot} \lesssim L_{\text{FIR}} \lesssim 10^{11} L_{\odot}$. To easily identify nearby companion galaxies, the bright *IRAS* sample is restricted to 87 objects with redshift range $0.008 \leq z \leq 0.018$ and Galactic latitude $\delta \geq |30^{\circ}|$. A control sample, selected from the CfA redshift-survey catalog, includes 90 objects matching the *IRAS* bright galaxy survey sample for distribution of isophotal diameter, redshift, and morphological type. From a search of nearby companion galaxies within 250 kpc in the second-generation Digitized Sky Survey (DSS-II), we find that the circumgalactic environments of bright *IRAS* galaxies contain more large companions than the galaxies in the optically selected control sample and are similar to those of Seyfert 2 galaxies. We find a weak correlation over a wide range of far-IR luminosity ($10^9 L_{\odot} \lesssim L_{\text{FIR}} \lesssim 10^{12.5} L_{\odot}$) between projected separation and L_{FIR} , which confirms a very close relationship between the star formation rate of a galaxy and the strength of gravitational perturbations. We also find that the far-IR colors depend on whether a source is isolated or interacting. Finally, we discuss the intrinsic difference between and evolution expectations for the bright *IRAS* galaxies and the control sample, as well as the relationship between starbursting and active galaxies.

Subject headings: galaxies: interactions — galaxies: starburst

1. INTRODUCTION

The *IRAS* bright galaxy survey (hereafter the BIRG survey) by Soifer et al. (1989) and Sanders et al. (1995) (southern extension) includes all galaxies brighter than 5.4 Jy at 60 μm . The bright *IRAS* galaxies are therefore, by definition, the brightest extragalactic objects in the sky at 60 μm . From this survey, we learned a wealth of astrophysical information: (1) the far-IR (FIR) emission dominates the total luminosity in a significant fraction of galaxies, and (2) at luminosity $\log(L_{\text{IR}}/L_{\odot}) \gtrsim 11$ (the so-called luminous infrared galaxies: LIRGs), IR-selected galaxies become more numerous than optically selected starburst and Seyfert galaxies of comparable bolometric luminosity. At luminosity $\log(L_{\text{IR}}/L_{\odot}) \gtrsim 12$, the so-called ultraluminous infrared galaxies (ULIRGs) exceed the space density of quasars by a factor of 1.5–2 (Sanders & Mirabel 1996; Sanders, Surace, & Ishida 1999).

A considerable number of studies suggest a strong relation between galaxy interactions and the highest IR luminosity. ULIRGs are often found to be interacting/merging systems (Sanders et al. 1999). However, the environment of moderately luminous infrared galaxies ($10^{10} L_{\odot} \leq L_{\text{FIR}} \leq 10^{11} L_{\odot}$, hereafter MIRGs), and LIRGs is not well known yet. In this paper, we study the circumgalactic environment of 87 galaxies from the BIRG survey, with luminosity range $10^{10} L_{\odot} \leq L_{\text{FIR}} \leq 10^{12} L_{\odot}$. The sample is composed of MIRGs and a few LIRGs. We also consider whether a correlation may be present between FIR properties and the projected separation of a BIRG and its nearest companion (§ 4.6). We then compare the BIRG environment with those of Seyfert 1s (Sy1s) and Seyfert 2s

(Sy2s) (§ 5.2). Finally, we discuss the implications of interaction-induced L_{FIR} enhancement for the secular evolution of galaxies and for the relationship between starbursting and active galaxies (§ 5). In the following discussion, we adopt a Hubble constant of $H_0 = 75 \text{ km s}^{-1} \text{ Mpc}^{-1}$.

2. SAMPLE SELECTION

2.1. Bright *IRAS* Sample

The bright *IRAS* sample consists of 87 objects and was compiled from the BIRG survey by Soifer et al. (1989) for the northern hemisphere and by Sanders et al. (1995) for the southern one. All objects with Galactic latitude $|b| \geq 30^{\circ}$ were included in the sample. In this way, we avoid sampling the Galactic plane, where a bias in the detection of companions is expected because of both absorption and crowding. We further restrict our selection to a volume-limited sample (redshift range $0.008 \leq z \leq 0.018$). A V/V_{max} test (Schmidt 1968) gives a value of 0.47 ± 0.05 (rms). Since the BIRG survey is highly complete, this sample is also expected to be complete.

The lower z limit (0.008) was chosen to avoid objects with very large angular size, while the upper z limit (0.018) was set to include the largest possible number of objects and at the same time to avoid very small angular sizes, especially for the companions that could be confused with stars (see § 3.1). It is important to point out that all the objects selected with the former restrictions lie in the luminosity range $10^{10} L_{\odot} \leq L_{\text{FIR}} \leq 10^{12} L_{\odot}$, with MIRGs being the wide majority ($\approx 92\%$ are MIRGs and 8% are LIRGs). The 60 μm luminosity (in ergs $\text{s}^{-1} \text{ \AA}^{-1}$) distribution and the L_{FIR}

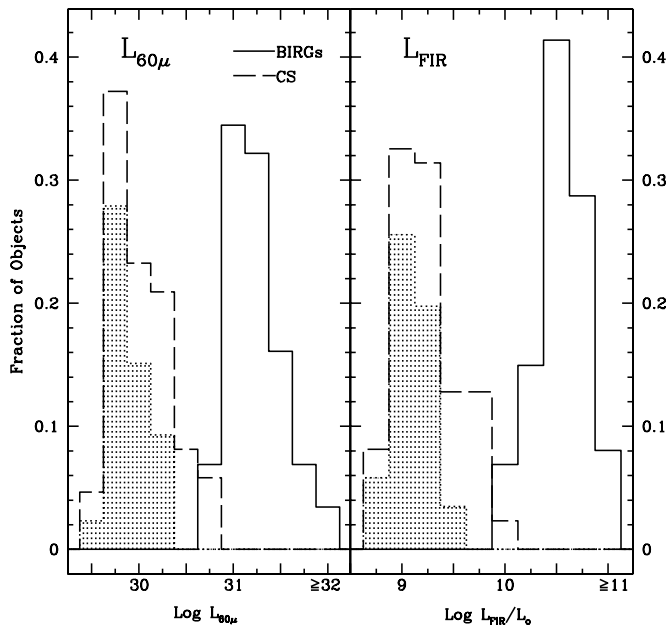


FIG. 1.—Luminosity at $60\ \mu\text{m}$ (in $\text{ergs s}^{-1}\ \text{\AA}^{-1}$) (left) and L_{FIR} (in solar units) (right) for BIRGs and CS galaxies. The solid line traces the distribution of the BIRG sample and the dashed line that of the CS, including detections as well as upper limits. The filled area identifies the distribution of objects from the CS whose specific luminosity at $60\ \mu\text{m}$ and L_{FIR} are known only as upper limits.

(in solar units) distribution of the BIRG sample are shown in the left and right panels of Figure 1, respectively.

2.2. Control Samples

The control sample (CS) for this study was randomly extracted from a list of more than 10,000 objects of the CfA Catalog (Huchra, Davis, & Latham 1983). This CS matches (1) the isophotal diameter, (2) the redshift, and (3) the Hubble morphological type distribution of the BIRG sample. Only objects with Galactic latitude $|b| \geq 30^\circ$ were included. The CS consists of 90 objects. A V/V_{max} test (Schmidt 1968) gives a value of 0.48 ± 0.04 (rms). The CS objects are low infrared emitters, as can be seen in Figure 1. Their flux at $60\ \mu\text{m}$ is usually much smaller than $5.4\ \text{Jy}$, and their luminosity at this wavelength is systematically smaller than the luminosity of the BIRGs. Objects without a detection are treated as upper limits, using the flux density limits of *IRAS*. The distribution of upper limits is shown by the filled histograms in Figure 1. The absolute B magnitude distribution was not matched. The B luminosity may be partially correlated with the IR luminosity, since both are enhanced through star formation processes. Therefore, any attempt to match the B luminosity could bias the CS toward galaxies with high infrared luminosity, which is what we want to avoid.

3. ANALYSIS

3.1. Identification of Galaxy Companions

As in previous environmental studies (Krongold, Dultzin-Hacyan, & Marziani 2001; Dultzin-Hacyan et al. 1999b), the search for galaxy companions was performed automatically in the second-generation Digitized Sky Survey (DSS-II) with the latest version (1998) of FOCAS (Faint

Object Classification and Analysis System; Jarvis & Tyson 1981) and was limited to galaxy companions that could be unambiguously distinguished from stars by the FOCAS algorithm. Each set of pixels with a flux value larger than the sky threshold is considered an object by FOCAS and can be classified as a galaxy or star only if its diameter is larger than 4 pixels. Since the scale of the DSS-II plates is $\approx 1''.0$ per pixel, the minimum angular size to which FOCAS is able to classify objects in the DSS-II is $\approx 4''$ (which corresponds to $\approx 1.4\ \text{kpc}$ of projected linear distance). However, we further restrict our search to companion galaxies of diameters $D_c \geq 5\ \text{kpc}$. With our methodology, we cannot study smaller objects because the distribution of companions is dominated by optical pairs (not physically associated; as pointed out in § 4.1, optical pairs are also the wide majority in the case of companion diameters between 5 and 10 kpc). A third limitation is that FOCAS classifies bright stars as galaxies, since they appear as extended objects due to scintillation effects. To avoid gross misclassifications, we checked by eye on the computer screen each object classified by FOCAS as a galaxy. Furthermore, borderline objects of marginally resolved appearance were not taken into account to also avoid second-order misclassifications. The effects of plate quality, the point-spread function, the sky background, and automatic identification and measurement of companion and background galaxies have been discussed in Krongold et al. (2001). They are not discussed again here; the same effects are still influencing the analysis of the DSS-II.

As was customary in many previous works (e.g., Dultzin-Hacyan et al. 1999a; Krongold et al. 2001), the fraction of objects with “physical” companions f_{phys} is taken as the fraction with one or more observed companions f_{obs} reduced by the fraction of galaxies with one or more optical companions (derived from Poisson distribution), namely, $f_{\text{phys}} = f_{\text{obs}} - f_{\text{opt}}$. The number of background galaxies expected to follow Poisson statistics has been obtained as described by Krongold et al. (2001).

4. RESULTS

4.1. Companions within $3D_o$

We looked for companions in a circular area with radius equal to 3 times the diameter of the central object ($3D_o$). Our results are summarized in Table 1.

Companion diameter $10\ \text{kpc} \geq D_c \geq 5\ \text{kpc}$.—Of the 87 BIRGs, $\approx 40\%$ have at least one companion within $3D_o$, versus 43% of the 90 objects of the CS. The expected number of optical companions from Poisson statistics is 36% for both the BIRGs and the CS. If optical companions are subtracted, f_{phys} is $\approx 4\%$ and 6.5% for the BIRGs and the CS, respectively. These results show that there is not a significant excess of companions between bright *IRAS* galaxies with respect to nonactive galaxies, if all companion galaxies with $5\ \text{kpc} \lesssim D_c \lesssim 10\ \text{kpc}$ are taken into account. However, this result should be viewed with caution, since $f_{\text{opt}} \gg f_{\text{phys}}$. A statistical approach is not appropriate in this companion size range. Any intersample difference can be proved as significant only if f_{phys} is estimated from redshift measurements for all companion galaxies.

Companion diameter $D_c \geq 10\ \text{kpc}$.—Of the 87 BIRGs, $\approx 58.4\%$ have at least one companion of diameter $D_c \geq 10\ \text{kpc}$ within a search radius $3D_o$, against $\approx 29\%$ of the 90

TABLE 1
FRACTION OF OBSERVED, OPTICAL, AND PHYSICAL COMPANIONS

| SAMPLE IDENTIFICATION | SAMPLE SIZE | FREQUENCY OF COMPANIONS (%) | | | SIGNIFICANCE ^a (%) |
|----------------------------------|-------------|-----------------------------|----------|----------|-------------------------------|
| | | Observed | Expected | Physical | |
| Companion Diameter ≥ 5 kpc | | | | | |
| BIRGs | 87 | 40.3 | 36.3 | 4 | ... |
| CS | 90 | 42.6 | 36.1 | 6.5 | Not significant |
| Companion Diameter ≥ 10 kpc | | | | | |
| BIRGs | 87 | 58.4 | 20 | 38.4 | ... |
| CS | 90 | 29 | 18.4 | 10.9 | 99.9 |

^a Statistical significance for the hypothesis that the listed samples are different from the BIRG sample.

objects of the CS. The expected number of optical companions from Poisson statistics is 20% and 18.4% for the BIRGs and the CS, respectively. If f_{opt} is subtracted, f_{phys} is $\approx 38.4\%$ and 10.9% for the BIRGs and the CS, respectively. These results show an excess of large companions ($D_c \geq 10$ kpc) in the bright *IRAS* galaxies with respect to nonactive galaxies. A χ^2 test gives a confidence level for this result of 99.9%.

4.2. Cumulative Distribution of the Nearest Companion in the BIRG Sample and in the CS

The search radius in all the cases was taken as 250 kpc of projected linear distance, beyond which we assumed a “nondetection.” The left-hand side of Figure 2 presents three panels with the cumulative distribution of the nearest companions (without correction for optical companions) up to a projected linear distance d_p of 140 kpc. The top panel shows the cumulative distribution of companions with diameter in the range $5 \text{ kpc} \leq D_c \leq 10 \text{ kpc}$, without subtraction of optical companions. The middle panel shows the cumulative distribution of companions with diameter $D_c \geq 10$ kpc, and the bottom panel shows the same distribution for companions with $D_c \geq 20$ kpc. The error bars on the CS frequencies were set with a “bootstrap” technique (Efron & Tibshirani 1993) by randomly resampling the CS galaxies into a large number (3000) of pseudo-CSs (i.e., we built 3000 pseudo-CSs of 90 randomly selected galaxies). The uncertainty on the companion frequency was set as equal to twice the standard deviation measured from the distribution of 3000 companion frequencies computed for each pseudo-CS. Comparing the environments of BIRGs and CS galaxies, it is found that there is a statistically significant excess of bright companions ($D_c \geq 10$ kpc) in the infrared emitters. For companion diameters $5 \text{ kpc} \leq D_c \leq 10 \text{ kpc}$, the samples show no significant difference.

4.3. Distribution of Objects with a Physical Companion

From Poisson statistics, we calculated f_{opt} at distances of 20 kpc, 40 kpc, etc. By subtracting this number from f_{obs} , we built the distribution of the nearest physical companions. The right-hand side of Figure 2 presents three panels with this distribution, up to $d_p \approx 140$ kpc. The top panel shows the distribution of physical companions with diameter in the range $5 \text{ kpc} \leq D_c \leq 10 \text{ kpc}$. The middle panel shows the distribution of physical companions with diameter $D_c \geq 10$ kpc. The bottom panel shows the distribution of physical companions with $D_c \geq 20$ kpc. In the latter case,

the surface density of objects above this diameter (20 kpc) is very low, and the probability of finding optical companions is negligible. Therefore, the cumulative f_{obs} is $\approx f_{\text{phys}}$. The error bars on the CS frequencies were again set with the bootstrap technique. As before, the results show a statistically significant excess of bright physical companions ($D_c \geq 10$ kpc) in the BIRGs. For companion diameters ≤ 10 kpc, there is no significant difference between the two samples.

4.4. BIRGs versus Sy1s and Sy2s

In order to study the difference between the environment of BIRGs and Sy1s and Sy2s, we used the data obtained for Seyfert environments by Dultzin-Hacyan et al. (1999b). The comparison is straightforward, since the z range of our

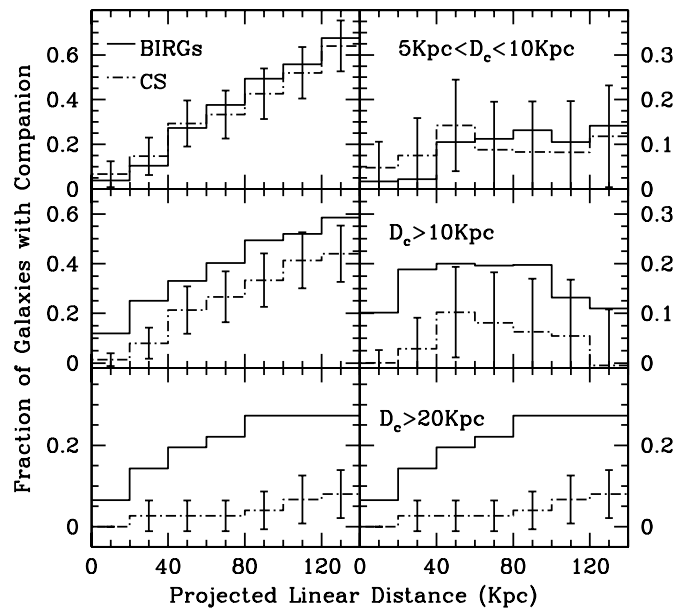


Fig. 2.—Left: Cumulative distributions of nearest observed companions to BIRGs binned over 20 kpc, with a projected linear distance limit of 140 kpc. Right: Distributions of “physical” companions (corrected for optical companions with Poisson statistics). The top panels show the distributions for galaxies with diameter $5 \text{ kpc} \leq D_c \leq 10 \text{ kpc}$, the middle panels show “bright” companion galaxies whose diameters are $D_c \geq 10 \text{ kpc}$, and the bottom panels show companions with $D_c \geq 20 \text{ kpc}$. The solid line corresponds to the BIRG sample, while the dot-dashed lines refer to the CS. The error bars on the CS are at a 2σ confidence level.

BIRG sample, search radius, and diameter limits are identical to the ones of the Sy2 sample of Dultzin-Hacyan et al. (1999b). The cumulative distribution for the projected distance d_p of the first observed companions for these objects is presented in Figure 3. The error bars in Figure 3 were set with the bootstrap technique, and are at a 2σ confidence level, as in Dultzin-Hacyan et al. (1999b). The bottom panel of Figure 3 shows that there is almost no difference in the distribution of first companion distances between the BIRGs and the Sy2s. On the contrary, the top panel shows that there is a statistically significant excess (a χ^2 test gives a confidence level of 99%) of companions in the BIRG sample with respect to Sy1s. A similar difference was found between Sy1s and Sy2s (Dultzin-Hacyan et al. 1999b).

4.5. Group Membership

We searched in the environment of our objects to determine whether they belonged to an association of galaxies. We considered any object with at least two companions with diameter $D_c \geq 10$ kpc within a circle of radius 200 kpc as a member of a group of galaxies. Of the 87 galaxies from the BIRG sample, 25% matched the former criteria (which corresponds to 43% of the BIRGs with a companion with $D_c \geq 10$ kpc). Only 4.3% of the CS objects were members of groups as defined here (which is 10% of the CS galaxies in pairs with $D_c \geq 10$ kpc). The results imply that BIRGs are more frequently found as members of groups than low IR emission galaxies.

Only $\approx 14\%$ of the objects in groups belong to compact groups of the Hickson Catalog (Hickson, Kindl, & Auman 1989) (this is $\approx 3.5\%$ of the 87 objects of the sample). We checked whether other BIRGs matched the Hickson criteria, but could not find any. BIRGs appear to preferentially

be members of groups, although of groups that are looser than Hickson's compact groups.

4.6. Interaction Strength and Infrared Emission

4.6.1. FIR Luminosity

Is FIR emission directly dependent on, or even proportional to, interaction strength? Our BIRG sample spans a limited range in L_{FIR} , 10^{10} – $10^{11} L_{\odot}$. In addition, several objects have companions whose angular separation is less than half the maximum width of the *IRAS* aperture. This implies that a biased correlation could arise just because, in the closest pairs, we are measuring the flux of two galaxies. Indeed, if the L_{FIR} of all small-separation ($\lesssim 1'$) systems is treated as an upper limit, there is no significant correlation between the projected linear separation d_p and L_{FIR} (and the correlation is significant if upper limits are treated as detections!).

A significant correlation appears only if a wider range of L_{FIR} is considered. We added to the BIRG sample data from three samples for which environmental data were available. We did not consider systems with a companion whose diameter was $5 \text{ kpc} \lesssim D_c \lesssim 15 \text{ kpc}$, since Figure 2 shows that most of them may be optical companions. The samples are the following:

1. Our CS.
2. The sample of “very luminous” IR galaxies by Wu et al. (1998), defined as galaxies with $\log L_{\text{IR}} \gtrsim 11.15$ in solar units.
3. The sample of LIRGs and ULIRGs selected by Sanders et al. (1999), which turn out to be composed of early- and late-stage mergers.

Figure 4 shows L_{FIR} versus d_p for the galaxies of the above samples. One has to consider three major limits to the data:

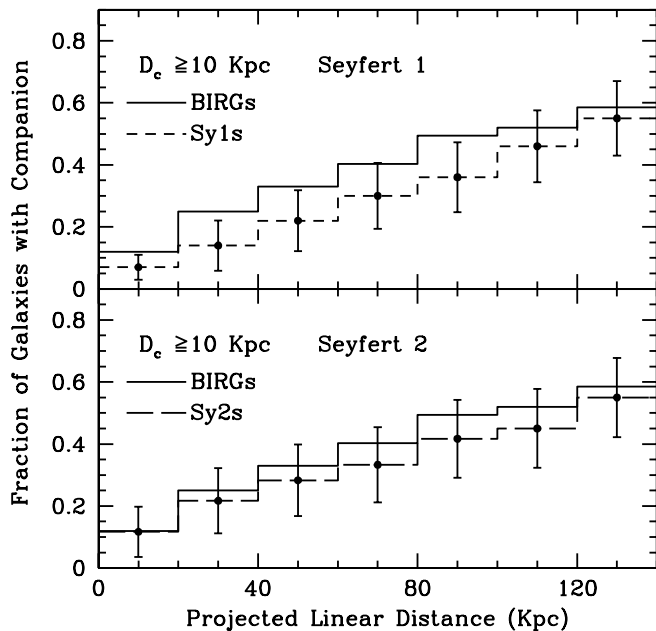


FIG. 3.—Distributions of the nearest companion with diameter $D_c \geq 10$ kpc, binned over 20 kpc, up to a projected linear distance of 140 kpc for Sy1s, Sy2s, and BIRGs. *Top*: BIRGs vs. Sy1s. *Bottom*: BIRGs vs. Sy2s. The solid line corresponds to the BIRG sample, while the dashed line refers to Sy1s in the top panel and Sy2s in the bottom panel. The error bars are set at a 2σ confidence level.

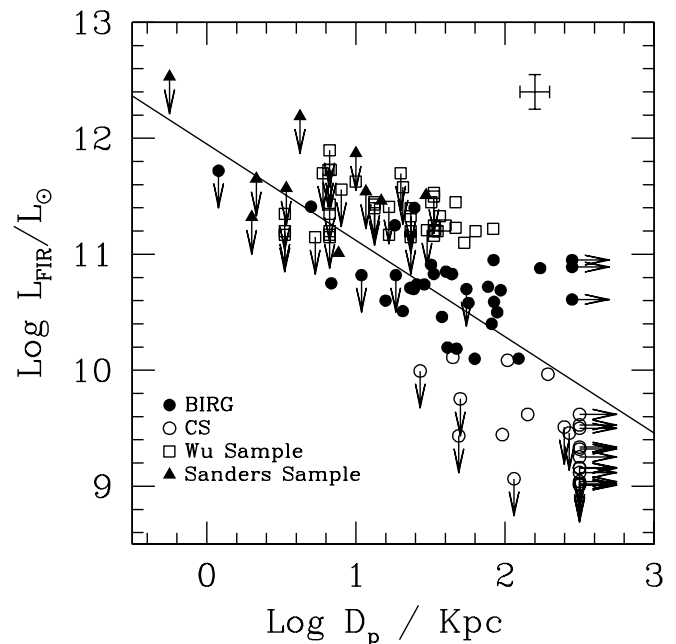


FIG. 4.—FIR luminosity L_{FIR} vs. projected separation d_p for BIRGs and CS galaxies with a bright companion, and for objects from Wu et al. (1998) and Sanders et al. (1999) samples. There are 107 objects in total. The solid line corresponds to the best fit.

1. For several objects, the aperture of the *IRAS* detectors was larger than the separation between the *IRAS* galaxy and the nearest companion, making it impossible to exclude a contribution of the companion to the measured L_{FIR} .

2. The search radius in the DSS-II was limited to 250 kpc. There are some objects (“isolated”) for which there are no companions of diameter larger than 5 kpc within this search radius.

3. For several CS galaxies, only upper limits to the fluxes are set. FIR fluxes were not available for 11 of 22 galaxies (either isolated or with a companion of $D_c \gtrsim 15$ kpc).

All these limitations introduce censoring to our data. We consider an upper limit to the L_{FIR} of the 11 CS objects that were not detected. For these objects, we take the flux-density limits in the four *IRAS* bands as upper limits to the source flux density. “Isolated objects” are treated as censored in the projected separation of the first companion, and a lower limit to d_p is set at our search radius of 250 kpc (“isolated” sources are the ones labeled with horizontal arrows in the bottom right side of Fig. 4). Of course, d_p values are lower limits to the true linear separation, which would be the most meaningful parameter to be correlated. However, the effect of chance projection is to horizontally spread the points toward the left in the diagram of Figure 4, but not to create a false correlation. For small- d_p objects, the infrared flux is measured for the system, and the flux for each galaxy is not available.

We therefore consider L_{FIR} for small-separation objects as an upper limit. We then apply the generalized Spearman rank correlation test with the inclusion of censored data. The correlation appears to be statistically significant, with a correlation coefficient $\lesssim -0.4$, considering small-separation objects as upper limits. The probability of the correlation being a chance correlation is $\lesssim 10^{-5}$. A best fit using Schmitt’s binning regression method yields the relationship $\log(L_{\text{FIR}}/L_{\odot}) \approx (-0.83 \pm 0.21) \log[d_p/(1 \text{ kpc})] + (11.95 \pm 0.33)$ (see Fig. 4). This result is confirmed by the presence of an analogous correlation between d_p and the specific luminosity at $60 \mu\text{m}$ (plot not shown).

4.6.2. FIR Colors

It is important to compare the IR properties of the galaxies with different strengths of interaction (and thus, with different projected separation d_p). To allow significant results to emerge in spite of the bias introduced by projection effects, we consider four interaction classes: (1) mergers (five Sanders objects and mergers from the BIRG sample), (2) strongly interacting systems (galaxies with companions closer than 30 kpc [$\log d_p < 1.5$, where d_p is in kiloparsecs]: five Sanders objects and the BIRG survey), (3) weakly interacting systems (galaxies with a companion beyond 30 kpc [$\log d_p > 1.5$]), and (4) isolated objects (objects without a companion within our search radius of 250 kpc). The objects in the BIRG sample and in the CS were split by interaction class.

Figure 5 shows the $F(60 \mu\text{m})/F(100 \mu\text{m})$ versus $F(12 \mu\text{m})/F(25 \mu\text{m})$ color-color diagram for the four interaction classes. Mergers and strongly interacting systems show higher values of $F(60 \mu\text{m})/F(100 \mu\text{m})$ and lower values of $F(12 \mu\text{m})/F(25 \mu\text{m})$, while isolated objects show lower values of $F(60 \mu\text{m})/F(100 \mu\text{m})$ and higher values of $F(12 \mu\text{m})/F(25 \mu\text{m})$. Figure 5 is divided into three regions. In the

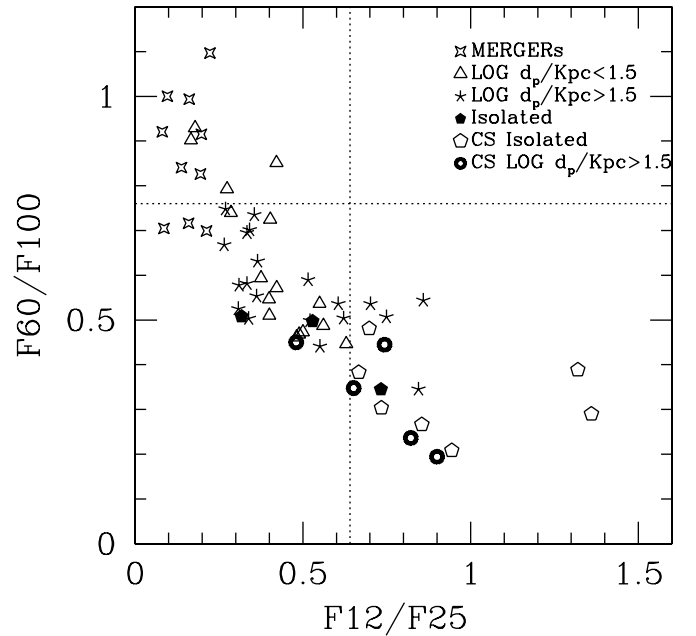


Fig. 5.—Color-color plot for objects in different interaction classes, split between BIRGs and the CS. The figure is divided into three regions. In the first one [$F(60 \mu\text{m})/F(100 \mu\text{m}) \gtrsim 0.75$ and $F(12 \mu\text{m})/F(25 \mu\text{m}) \lesssim 0.65$], almost all objects are mergers and strongly interacting. In the second region [$F(60 \mu\text{m})/F(100 \mu\text{m}) \lesssim 0.75$ and $F(12 \mu\text{m})/F(25 \mu\text{m}) \lesssim 0.65$], there is an agglomeration of objects of all interaction classes. The third region [$F(60 \mu\text{m})/F(100 \mu\text{m}) \lesssim 0.75$ and $F(12 \mu\text{m})/F(25 \mu\text{m}) \gtrsim 0.65$] shows only objects with a companion beyond 30 kpc and isolated galaxies.

first one [$F(60 \mu\text{m})/F(100 \mu\text{m}) \gtrsim 0.75$ and $F(12 \mu\text{m})/F(25 \mu\text{m}) \lesssim 0.65$], almost all objects are mergers and strongly interacting. In the second region [$F(60 \mu\text{m})/F(100 \mu\text{m}) \lesssim 0.75$ and $F(12 \mu\text{m})/F(25 \mu\text{m}) \lesssim 0.65$], there is an agglomeration of objects of all interaction classes. However, the three mergers in this region are near the border of the first region, and their IR colors are very close to the values of the first region mergers. The third region [$F(60 \mu\text{m})/F(100 \mu\text{m}) \lesssim 0.75$ and $F(12 \mu\text{m})/F(25 \mu\text{m}) \gtrsim 0.65$] shows only objects with a companion beyond 30 kpc, and isolated galaxies.

4.6.3. Overall Properties

Table 2 reports average and sample standard deviation values of the parameters considered in our analysis (col. [1]) for different interaction strength classes. Columns (2)–(5) report sample average and sample standard deviation for isolated CS galaxies and BIRGs ($d_p \gtrsim 250$ kpc). Columns (6)–(9) report values for weakly interacting BIRGs and CS galaxies with $d_p \gtrsim 30$ kpc. The next columns list the sample average and standard deviation for the BIRG sample for the remaining two interaction classes: strongly interacting and mergers (there are no CS galaxies either with $d_p \lesssim 30$ kpc or in mergers). The last four rows provide standard estimates of star formation related parameters: (1) the star formation rate (SFR), which was computed from L_{FIR} using the standard relationship $\text{SFR} \approx 4.5 \times 10^{-44} L_{\text{FIR,ergs s}^{-1}} M_{\odot} \text{ yr}^{-1}$ (Kennicutt 1998); (2) molecular hydrogen mass M_{H_2} (collected from various sources in literature and available for 41 objects); (3) the ratio $L_{\text{FIR}}/M_{\text{H}_2}$; and (4) the depletion time in years, simply defined as the assumed molecular hydrogen gas mass over the SFR, $\tau_{\text{H}_2} = M_{\text{H}_2}/\text{SFR}$.

TABLE 2
FIR PROPERTIES FOR GALAXIES WITH DIFFERENT INTERACTION STRENGTHS

| PARAMETER (1) | ISOLATED | | | | SEPARATION > 30 kpc | | | | SEPARATION < 30 kpc | | Mergers | |
|---|-----------|-----------|--------------|-----------|---------------------|-----------|--------------|-----------|---------------------|------------|-----------------|------------|
| | CS (2) | SD (3) | BIRGs (4) | SD (5) | CS (6) | SD (7) | BIRGs (8) | SD (9) | BIRGs (10) | SD (11) | Mergers (12) | SD (13) |
| Number of objects..... | 11 | ... | 3 | ... | 11 | ... | 20 | ... | 16 | ... | 10 | ... |
| $\langle d_p \rangle$ (kpc)..... | > 250 | ... | > 250 | ... | 111.73 | 71.50 | 66.94 | 35.05 | 18.20 | 7.42 | 1.81 | 1.17 |
| $\langle L_{\text{FIR}} \rangle$ ($10^{10} L_{\odot}$)..... | 0.21 | 0.13 | 6.92 | 2.53 | 0.92 | 0.47 | 3.83 | 2.30 | 16.8 | 18.8 | 71.6 | 103.2 |
| $\langle L_{12\mu\text{m}} \rangle$ ($10^{30} \text{ ergs}^{-1} \text{ Hz}^{-1}$)..... | 0.27 | 0.15 | 1.35 | 0.20 | 0.34 | 0.21 | 1.19 | 0.71 | 5.16 | 8.76 | 9.43 | 1.99 |
| $\langle L_{25\mu\text{m}} \rangle$ ($10^{30} \text{ ergs}^{-1} \text{ Hz}^{-1}$)..... | 0.29 | 0.12 | 2.98 | 1.71 | 0.39 | 0.30 | 2.61 | 1.44 | 14.6 | 22.2 | 48.6 | 88.4 |
| $\langle L_{60\mu\text{m}} \rangle$ ($10^{30} \text{ ergs}^{-1} \text{ Hz}^{-1}$)..... | 1.02 | 0.51 | 19.4 | 8.70 | 3.38 | 2.80 | 20.2 | 10.5 | 70.3 | 67.7 | 275.1 | 374.2 |
| $\langle L_{100\mu\text{m}} \rangle$ ($10^{30} \text{ ergs}^{-1} \text{ Hz}^{-1}$)..... | 3.40 | 2.27 | 42.3 | 13.1 | 9.85 | 6.84 | 37.1 | 22.0 | 103.2 | 79.1 | 285.3 | 344.4 |
| $\langle F(12\mu\text{m})/F(25\mu\text{m}) \rangle$ | 0.94 | 0.29 | 0.53 | 0.21 | 0.72 | 0.16 | 0.48 | 0.19 | 0.41 | 0.13 | 0.16 | 0.05 |
| $\langle F(60\mu\text{m})/F(100\mu\text{m}) \rangle$ | 0.33 | 0.09 | 0.45 | 0.09 | 0.34 | 0.12 | 0.57 | 0.10 | 0.63 | 0.17 | 0.87 | 0.14 |
| $\langle M_{\text{H}_2} \rangle$ ($10^9 M_{\odot}$)..... | 3.77 | 1.68 | 2.95 | NA | 7.12 | 2.11 | 6.40 | 5.89 | 7.55 | 6.81 | 9.60 | 9.04 |
| $\langle L_{\text{FIR}}/M_{\text{H}_2} \rangle$ (L_{\odot}/M_{\odot})..... | 0.52 | 0.42 | 26.30 | NA | 0.85 | 0.53 | 13.56 | 12.65 | 31.47 | 35.94 | 118.0 | 105.77 |
| $\langle \text{SFR} \rangle^a$ ($M_{\odot} \text{ yr}^{-1}$)..... | 0.36 | 0.23 | 12.10 | 4.42 | 1.45 | 1.15 | 6.71 | 4.03 | 29.56 | 32.95 | 125.34 | 180.09 |
| $\langle \tau_{\text{H}_2} \rangle^b$ (10^9 yr)..... | 19.6 | 17.9 | 0.22 | NA | 8.39 | 5.22 | 0.91 | 0.86 | 0.51 | 0.59 | 0.09 | 0.08 |

NOTE.—Columns headed by SD are the standard deviation, and NA in a cell means that the value was not available.

^a The quantity $\text{SFR} \approx 4.5 \times 10^{-44} L_{\text{FIR,ergs}^{-1}} M_{\odot} \text{ yr}^{-1}$ (Kennicutt 1998).

^b The quantity $\tau_{\text{H}_2} = M_{\text{H}_2}/\text{SFR}$.

There is a clear continuity of FIR properties and the SFR from isolated objects to mergers (except for the three isolated BIRGs, but see below). The quantity L_{FIR} increases with the interaction strength as indicated by our correlation analysis. Systematic differences in FIR color are also appreciable. The depletion time is $\lesssim 10^9$ yr for *all* interaction classes (including isolated objects) in the BIRG sample. In the CS objects, $\tau_{\text{H}_2} \sim 10^{10}$ yr, comparable to the Hubble time. There is a monotonic trend from isolated galaxies to mergers in terms of increasing SFR and decreasing τ_{H_2} , but it is noteworthy that M_{H_2} is not statistically different in the various interaction classes.

Isolated objects from the CS and isolated objects from the BIRG sample have impressively different L_{FIR} . This apparent contradiction needs an explanation. There are only three isolated BIRGs. NGC 5937, NGC 7083, and NGC 5936 did not show a companion larger than 5 kpc in the DSS-II within 250 kpc. However, all of these galaxies present peculiarities. (1) NGC 5937 has a distorted morphology, and it may have a loop of gas that could be a signature of interaction. (2) NGC 7083 is a barred Sc galaxy that hosts a LINER. It looks perturbed because of an off-centered loop. (3) NGC 5936 has a highly distorted morphology, which may be indicative of recent interaction. These galaxies may have been disturbed by the presence of a small companion disrupted or projected over the main galaxy. Isolated CS galaxies do not show distortions or peculiarities that could make them special objects in terms of morphology or interaction.

5. DISCUSSION

The percentage of companion galaxies within $3D_o$ and the distributions of observed and physical companions show a highly significant excess for the BIRGs. The difference between BIRGs and CS galaxies is especially striking if large companions with $D_c \gtrsim 20$ kpc are considered (the BIRGs have 3–4 times more companions within ≈ 140 kpc; strongly interacting systems in the CS may be $\lesssim 1\%$). Our results also indicate a direct relationship between interaction and

enhancement of IR emission. We have considered a very large range in L_{FIR} , $\sim 10^{8.5}–10^{12.5} L_{\odot}$, which is unprecedented and probably sufficient to overcome the bias introduced by random projection of separation. This may explain why, with some notable exceptions (e.g. Sanders & Mirabel 1996, and references therein), several previous analyses did not find any convincing correlation between d_p and L_{FIR} among interacting galaxies. Our result extends to a lower L_{FIR} range and quantifies results that were known qualitatively for LIRGs and ULIRGs (Sanders et al. 1999).

5.1. Implications for Star Formation

An increase in L_{FIR} can be observed across a sequence from isolated galaxies to strongly interacting systems. Color variations are consistent with the emergence of an FIR continuum component whose luminosity and colors are correlated. This component can be associated with thermal reradiation by the continuum emission of the dust of hot stars. In the most extreme cases of isolated CS galaxies, we may have only a cold cirrus component, $T \sim 20$ K. At the other end of the FIR color-color diagram, a “hot” component peaking around 100–60 μm may become prominent. The increase in L_{FIR} can be largely ascribed to an increase in the SFR, as shown in many previous studies (Kennicutt 1998, and references therein; Sauvage & Thuan 1992). For the “hottest” sources [$F(25\mu\text{m})/F(60\mu\text{m}) \gtrsim 0.2$], however, the reprocessed continuum may be due to a nonthermal source (de Grijs et al. 1992).

The difference in L_{FIR} and $L_{\text{FIR}}/M_{\text{H}_2}$ (a factor of more than 100 from mergers to isolated CS objects; see Table 2) suggests that strong interactions ($d_p \lesssim 30$ kpc) are a necessary and sufficient condition for an extreme SFR and for a “starburst” (defined as star formation that cannot be maintained over the Hubble time), at least for the galaxies of our sample (this result may not be generally true if not all mergers of gas-rich galaxies are luminous in the infrared). A companion that has approached to less than 30 kpc from a galaxy may need a time $\gtrsim 3 \times 10^8 d_{30\text{kpc}} v_{100\text{km s}^{-1}}^{-1}$ yr to move beyond this distance. The mean depletion time for strongly interacting galaxies is $\approx 5 \times 10^8$ yr (Table 2). In this case, the

interaction time and τ_{H_2} are comparable. This means that a galaxy may exhaust its gas before an interaction episode is over, on a time much less than the Hubble time.

On the other hand, the SFRs of weakly interacting galaxies (CS galaxies with $d_p \gtrsim 30$ kpc) do not show values that may be considered extraordinary (SFR $\approx 0.52 M_\odot \text{ yr}^{-1}$). For objects whose companion is separated by $d_p \gtrsim 30$ kpc, the average d_p is approximately 112 and 67 kpc in the CS and in the BIRG sample, respectively. The SFR is ≈ 10 times larger in the BIRG sample than in the CS. This is consistent with tidal forces ($\propto d_p^{-3}$) driving the SFR increase. A weak interaction may produce a moderate enhancement of the SFR of a galaxy but not lead to dramatic effects on its secular evolution. An important implication of our results is that at least part of the large dispersion (a factor of ~ 10) for the SFR in galaxies of a particular morphological type (see Kennicutt 1998) may be explained by weak interactions (c.f. Hernández Toledo, Dultzin-Hacyan, & Sulentic 2001).

5.2. Relationship between Star-forming and Seyfert Galaxies

Our work and many previous ones leave no doubt that gravitational interaction leads to an increase of the SFR in gas-rich galaxies. Less clear is the relationship between interaction and the occurrence of nonthermal nuclear activity. In the simplest scheme of Seyfert unification, Sy1s and Sy2s are different because of orientation (see, e.g., Antonucci 1993 for a review): a molecular torus makes obscuration a major factor in the appearance of an active nucleus. However, interaction may be a factor leading to the formation of the obscuring torus itself and to the production of extensive circumnuclear star formation. A significant role of interaction introduces an additional degree of freedom (Dultzin-Hacyan et al. 1999b) related to environment and, in a broad sense, evolution.

5.2.1. The Environment of Seyfert Galaxies

The main question is, then: What is the environment of Seyfert galaxies? The most recent works have found a positive excess of large companions among Sy2s but not among Sy1s (Dultzin-Hacyan et al. 1999b; Laurikainen & Salo 1995; de Robertis, Yee, & Hayhoe 1998). This challenges previous results suggesting an excess without differences between Sy1s and Sy2s (Dahari 1984; Rafanelli, Violato, & Baruffolo 1995). Problems here may arise because of intrinsic inhomogeneity in the discovery techniques of Sy2s, as discussed explicitly by Marziani (1991). In addition, it has to be taken into account that discovery methods for Sy2s such as the UV excess and the FIR color are sensitive to enhanced star formation. For instance, Schmitt et al. (2001) selected an FIR flux limited sample on the basis of FIR color. They found that $31\% \pm 10\%$ of Sy1s and $28\% \pm 7\%$ of Sy2s have companions (optical + physical) within three diameters. These frequencies are very similar to the frequency found for Sy2s by Dultzin-Hacyan et al. (1999b) (companion diameter ≥ 10 kpc within 60 kpc, the case most similar to the one considered by Schmitt et al. 2001). By introducing a bias in favor of star-forming Sy1s, their selection criterion may have simply *increased* the fraction of interacting Sy1s (Dultzin-Hacyan et al. 1999b found 21%) with respect to Sy2s. As can be seen below, almost all active galactic nuclei (AGNs) from the BIRG sample show evidence of significant star formation *and* belong to interacting systems.

Since an excess is found from uniformly distributed samples (Dultzin-Hacyan et al. 1999b) and also for a Seyfert sample selected from the CfA redshift survey (de Robertis et al. 1998), we consider *an excess of bright companions among Sy2s and no excess among Sy1s with respect to a suitably chosen CS of nonactive galaxies* as the most accurate representation of the Seyfert environment.

5.3. Star-forming and Seyfert Galaxies: An Evolutionary Sequence?

The result of this paper that is relevant at this point is that BIRGs seem to have, to a high confidence level, more large and close companions ($D \geq 10$ kpc, $d \leq 60$ kpc) than Sy1s and seem to be similar in their environment to Sy2s (c.f. Dultzin-Hacyan et al. 1999b). This statistical result gives support to a scheme that several works have considered (Heckman et al. 1989, and references therein; Sanders et al. 1988). The scheme is an evolutionary sequence for AGNs driven by interaction,

$$\text{interaction} \Rightarrow \text{starburst} \rightarrow \text{Seyfert 2} \Leftrightarrow \text{Seyfert 1}, \quad (1)$$

where the double arrow indicates that Sy1s and Sy2s may actually be the same kind of objects seen in different orientations. There are several lines of (admittedly circumstantial) evidence that also support this simple evolutionary path. First, the contribution of thermal emission to the bolometric luminosity appears to decrease along the sequence (Dultzin-Hacyan & Ruano 1996). Sy1 nuclei have been revealed in several evolved mergers (for instance, see Rafanelli et al. 1993). Second, there are several active galaxies in the BIRG sample. Of 87 galaxies, 17% host a Sy2 nucleus (15 objects), but only 2.5% host a Sy1 nucleus (two objects). There is no statistical difference between the L_{FIR} of active and nonactive galaxies, except for a slightly higher value in the Sy1 objects. The value of $F(25 \mu\text{m})/F(60 \mu\text{m})$ for Sy2s is ≈ 0.18 , and for Sy1s, ≈ 0.20 , compared to ≈ 0.13 for nonactive galaxies. The quantity $F(25 \mu\text{m})/F(60 \mu\text{m})$ is larger in Sy1s and Sy2s due to the contribution to the continuum of a nonthermal source (de Grijp et al. 1992). Estimating in a careful way the ratio of thermal to nonthermal emission for the BIRGs is not possible from published data. However, 73% of the Sy2s (11 of 15) show evidence of significant star formation (there is evidence of a circumnuclear starburst in 45% of the star-forming Sy2s). In addition, the two BIRG Sy1s show evidence of a circumnuclear starburst. (This makes selecting samples of Sy1s and Sy2s from L_{FIR} even more improper for environmental studies than selecting them from catalogs!)

The evolutionary sequence outlined above can be understood in three different ways:

1. It can be read as a sequence of obscuration properties: (a) fully obscured Sy1s (i.e., seen as a Sy2 from all viewing angles), (b) obscuration dependent on the viewing angle of the Sy1s (the Sy1 and Sy2 “unification” scenario), and (c) almost fully unobscured Sy1s.

2. It can be a sequence of AGN power; a possibility is that the accretion rate may be insufficient to maintain a broad-line region (BLR) in some Sy2s.

3. A low power may also occur in its earlier stages, just because the central black hole is of rather low mass, maybe because the black hole *was not originally present*.

A wealth of X-ray data show that most Sy2s are consistent with an AGN X-ray spectrum increasingly less absorbed at energies $\gtrsim 5$ keV. This means that an AGN has already been switched on in many, if not all, Sy2s (Moran et al. 2001; Matt 1997). This result supports the obscuration sequence (since the power of the AGN will roughly be the same in different types). In this scheme, Sy2s may appear as the low-luminosity analogs of ULIRGs, which have been suggested to be precursors of quasars.

Tran (2001) studied a sample of Sy2s to determine how many of them were obscured Sy1s, i.e., showed a hidden BLR (HBLR) in polarized light. He concluded that non-HBLR Sy2s are not more obscured than HBLR Sy2s, but less powerful AGNs. This result goes against the obscuration scenario and favors the AGN power scenario (points 2 and 3). Gu, Dultzin-Hacyan, & de Diego (2001) studied the properties of 51 Sy2s with evidence of a high circumnuclear SFR. They found that while Sy2s with an HBLR have similar infrared-radio properties as Sy1s, Sy2s without an HBLR have properties similar to starbursts. These results can be straightforwardly understood in the context of an evolutionary scheme. While objects without an HBLR are “younger” Sy1s (whether very obscured or with very low AGN power), Sy2s with an HBLR are “young” Sy1s that may keep forming stars in their nuclear region but that are less obscured or have higher AGN power.

Obscuration, low accretion, or small black hole mass could therefore be the main physical factors behind any evolutionary sequence. However, we think that there is currently not enough evidence to decide in favor of one of these factors.

5.3.1. *Environmental Effects as Drivers of Any Evolutionary Sequence*

The time needed for Sy1s to emerge (whether as unobscured or as high-power AGNs) could be longer than the escape time of an unbound companion from the very close environment or comparable to the timescale needed for an evolved merger ($\sim 10^9$ yr). This naturally explains why starbursts and Sy2s are found more often with closer companions.

For AGN triggering in a gas-rich galaxy, the occurrence of a tidal perturbation may be more relevant than its duration (Keel 1996). A hyperbolic encounter may well trigger a radial flow in the innermost regions of a gas-rich galaxy. The time needed by the companion to move away by 30 kpc is $\sim 1.0 \times 10^8 d_{30 \text{ kpc}} \Delta v_{300 \text{ km s}^{-1}}^{-1}$ yr. The timescale for a clump of gas to fall from the outer regions of the nucleus (a few hundreds of parsecs) to the inner central parsec is $\gtrsim 0.1$ Gyr (Bekki 2000), and this can be considered a lower limit to the time needed for the onset of the active nucleus. Therefore, a hyperbolic encounter with moderate Δv_r can be such that the companion escapes from the close vicinity (≈ 60 kpc) of the Seyfert galaxy, leaving a noninteracting Sy1 nucleus. If obscuration is significant, or if the AGN power is small (because of low accretion rate or an undermassive central black hole), then a longer timescale may be necessary before a Sy1 nucleus is actually detected. While BIRGs and Sy2 galaxies have richer environments than Sy1s at distances $\lesssim 60$ kpc, the cumulative distribution of the projected separation for the first companion (Fig. 3) shows that the environmental difference for Sy1s with respect to Sy2s and BIRGs decreases dramatically beyond ≈ 120 kpc. This

means that, while Sy2s and BIRGs have close companions, Sy1s do have companions, but at higher distances ($d_p \gtrsim 100$ kpc). Sy1s do not show close companions simply because any activity-triggering interaction has taken place in the past, and on average, Sy1s would not be considered interacting following our statistical criterions.

The limitations of our analysis regarding small companion galaxies ($D_c \lesssim 10$ kpc) leave open other likely possibilities to account for type 1 activity. It has been proposed that Sy1s may be the result of a “minor merger,” which purportedly may lead to no dramatic star formation close to the center of the galaxy and hence to heavy obscuration (de Robertis et al. 1998; Taniguchi 1999). Minor merger N -body simulations show that they produce disturbances in the morphology of the larger galaxies in the first gigayear of the onset of the merger, but do not destroy the galactic disk (Walker, Mihos, & Hernquist 1996). Corbin (2000) did not find higher levels of asymmetry in Seyfert galaxies than in normal galaxies (in agreement with our work, he found that the most asymmetric galaxies were interacting systems with H II–like spectra). He concluded that, if minor mergers trigger AGNs, they appear to do so only in the late stages of the mergers (~ 1 Gyr after the merger onset). Minor mergers also boost the star formation of the larger galaxy, but this process is not necessarily very dramatic (the induced SFR may be as low as $\approx 2 M_\odot \text{ yr}^{-1}$), especially after the first 0.5 Gyr (Rudnick, Rix, & Kennicutt 2000).

The previous mechanisms suggest a revision that complements the unification scheme for Seyfert galaxies and favors the idea of a long timescale to let type 1 AGNs emerge. It is interesting to stress that times for the onset of this kind of activity are in agreement with the time needed to let any unbound companion fly at least a few tens of kiloparsecs or to have a full or a “minor” merger (~ 1 Gyr).

5.3.2. *The Unlikely Alternative: No Effect on AGN Triggering by Tidal Forces*

An alternative interpretation for the environmental results for BIRGs, Sy2s, and Sy1s is that interactions may trigger only high SFR but no nuclear, nonthermal activity. Sy2s may show an interaction-induced enhancement in the SFR, as do any other interacting galaxies, at least on average. This implies two populations of Sy2s (Storchi-Bergmann et al. 2001):

Interacting Sy2s with high SFR.—The morphology of these galaxies should be distorted because of the interaction, and the interaction could be responsible for the obscuring torus of dust, if it exists. The properties of these Sy2 galaxies should be similar to those of star-forming galaxies.

Sy2s isolated and without any circumnuclear starburst.—Due to the lack of interactions, the morphology of these objects should be very symmetric, without distortions, and as Sy1s, these galaxies should not have any excess of companions when compared to normal galaxies.

If this distinction is correct, strong interactions and non-thermal activity could be fully unrelated phenomena (Corbin 2000). The issue would suffer a 30 year setback. The crucial test is then whether the excess of interacting Sy2s with respect to normal galaxies is real for a *complete sample of Sy2s*. If not, then there would be no support for a relationship between interaction and Seyfert-type activity. If

yes, then the evolutionary sequence above may be appropriate. Defining a complete sample of Sy2s is tricky, but as already noted, the results based on a limited CfA sample suggest that the difference between Sy2s and Sy1s may not be due to sample selection biases. As noted earlier, the value of $F(25\ \mu\text{m})/F(60\ \mu\text{m})$ for Sy2s is ≈ 0.18 , and for Sy1s ≈ 0.20 . This result argues against two Sy2 populations, since interacting Sy2s with a high SFR (such as the Sy2s of the BIRG sample) should have properties more similar to star-forming galaxies, rather than to Sy1s [and thus, lower $F(25\ \mu\text{m})/F(60\ \mu\text{m})$ ratios].

6. CONCLUSIONS

We studied the environments of bright *IRAS* galaxies and compared them with those of low FIR emitters, as well as to those of Seyfert 1 and 2 galaxies. We found that, on average, BIRGs are more often in interaction, and their “interaction strength” is higher than in a sample of optically selected galaxies. Our results show a weak anticorrelation between the projected separation of the first companion and the FIR luminosity of a galaxy, which means an anticorrelation

between d_p and the SFR. This extends previous results for luminous and ultraluminous FIR galaxies. The FIR properties show a clear and smooth continuity as a function of interaction strength, going from very low FIR activity in isolated normal galaxies to very high activity in mergers. A consequence is that the FIR luminosity function as a function of morphological types is meaningful only for strictly isolated, unperturbed systems. The similar environment found for Sy2s and BIRGs supports the possibility of an evolutionary link between starbursts, Sy2s, and Sy1s.

This research has made use of the Digitized Sky Surveys that were produced at the Space Telescope Science Institute, under US government grant NAG W-2166, and of the NASA/IPAC Extragalactic Database (NED), which is operated by the Jet Propulsion Laboratory, California Institute of Technology, under contract with the National Aeronautics and Space Administration. P. M. acknowledges financial support from grant Cofin 2000-02-004. Y. K. acknowledges financial support from grant PAEP 201304. D. D. H. acknowledges financial support from grant IN 115599 PAPIIT DGAPA-UNAM.

REFERENCES

- Antonucci, R. 1993, *ARA&A*, 31, 473
 Bekki, K. 2000, *ApJ*, 545, 753
 Corbin, M. R. 2000, *ApJ*, 536, L73
 Dahari, O. 1984, *AJ*, 89, 966
 de Grijp, M. H. K., Miley, G. K., Goudfroij, P., & Lub, J. 1992, *A&AS*, 96, 389
 de Robertis, M. M., Yee, H. K. C., & Hayhoe, K. 1998, *ApJ*, 496, 93
 Dultzin-Hacyan, D., Guridi, I. F., Krongold, Y., & Marziani, P. 1999a, in *IAU Symp. 186, Galaxy Interactions at Low and High Redshift*, ed. J. Barnes & D. B. Sanders (Dordrecht: Kluwer), 329
 Dultzin-Hacyan, D., Krongold, Y., Fuentes-Guridi, I., & Marziani, P. 1999b, *ApJ*, 513, L111
 Dultzin-Hacyan, D., & Ruano, C. 1996, *A&A*, 305, 719
 Efron, B., & Tibshirani, R. J. 1993, *An Introduction to the Bootstrap* (New York: Chapman & Hall)
 Gu, Q., Dultzin-Hacyan, D., & de Diego, J. A. 2001, *Rev. Mexicana Astron. Astrofis.*, 37, 3
 Heckman, T. M., Blitz, L., Wilson, A. S., Armus, L., & Miley, G. K. 1989, *ApJ*, 342, 735
 Hernández Toledo, H. M., Dultzin-Hacyan, D., & Sulentic, J. W. 2001, *AJ*, 121, 1319
 Hickson, P., Kindl, E., & Auman, J. R. 1989, *ApJS*, 70, 687
 Huchra, J., Davis, M., & Latham, D. 1983, *Smithsonian Center for Astrophysics Catalog* (Cambridge: Cambridge Univ. Press)
 Jarvis, J. F., & Tyson, J. A. 1981, *AJ*, 86, 476
 Keel, W. C. 1996, *AJ*, 111, 696
 Kennicutt, R. C. 1998, *ARA&A*, 36, 189
 Krongold, Y., Dultzin-Hacyan, D., & Marziani, P. 2001, *AJ*, 121, 702
 Laurikainen, E., & Salo, H. 1995, *A&A*, 293, 683
 Marziani, P. 1991, Ph.D. thesis, International School for Advanced Studies, Trieste
 Matt, G. 1997, *Mem. Soc. Astron. Italiana*, 68, 127
 Moran, E. C., Kay, L. E., Davis, M., Filippenko, A. V., & Barth, A. J. 2001, *ApJ*, 556, L75
 Rafanelli, P., Marziani, P., Birkle, K., & Thiele, U. 1993, *A&A*, 275, 451
 Rafanelli, P., Violato, M., & Baruffolo, A. 1995, *AJ*, 109, 1546
 Rudnick, G., Rix, H., & Kennicutt, R. C. 2000, *ApJ*, 538, 569
 Sanders, D. B., Egami, E., Lipari, S., Mirabel, I. F., & Soifer, B. T. 1995, *AJ*, 110, 1993
 Sanders, D. B., & Mirabel, I. F. 1996, *ARA&A*, 34, 749
 Sanders, D. B., Soifer, B. T., Elias, J. H., Madore, B. F., Matthews, K., Neugebauer, G., & Scoville, N. Z. 1988, *ApJ*, 325, 74
 Sanders, D. B., Surace, J. A., & Ishida, C. M. 1999, in *IAU Symp. 186, Galaxy Interactions at Low and High Redshift*, ed. J. Barnes & D. B. Sanders (Dordrecht: Kluwer), 289
 Sauvage, M., & Thuan, T. X. 1992, *ApJ*, 396, L69
 Schmidt, M. 1968, *ApJ*, 151, 393
 Schmitt, H. R., Antonucci, R. R. J., Ulvestad, J. S., Kinney, A. L., Clarke, C. J., & Pringle, J. E. 2001, *ApJ*, 555, 663
 Soifer, B. T., Boehmer, L., Neugebauer, G., & Sanders, D. B. 1989, *AJ*, 98, 766
 Storchi-Bergmann, T., González Delgado, R. M., Schmitt, H. R., Cid Fernandes, R., & Heckman, T. 2001, *ApJ*, 559, 147
 Taniguchi, Y. 1999, *ApJ*, 524, 65
 Tran, H. D. 2001, *ApJ*, 554, L19
 Walker, I. R., Mihos, J. C., & Hernquist, L. 1996, *ApJ*, 460, 121
 Wu, H., Zou, Z. L., Xia, X. Y., & Deng, Z. G. 1998, *A&AS*, 132, 181